Uncertainty Assessment of Optical Distance Measurements at Micrometer Level Accuracy for Long-Range Applications

Joffray Guillory, Maylis Teyssendier de La Serve, Daniel E Truong, Christophe Alexandre, Jean-Pierre Wallerand

Uncertainty assessment of optical distance measurements at micrometer level accuracy for long-range applications

J. Guillory, M. Teyssendier de la Serve, D. Truong, C. Alexandre, and J.-P. Wallerand

***Abstract*—We have developed a transportable distance meter based on a 1550 nm laser diode that is intensity modulated at 5 GHz. This fiber-based prototype is realized using telecommunication components that are reliable, largely available and affordable. We have identified and quantified the different sources of error when measuring with this technique a distance between two positions of a same reflector. Minimizing these errors and evaluating their uncertainties lead to a global uncertainty of 4 µm (k=1) up to 1 km. This value does not include the additional errors caused by the evaluation of the atmospheric parameters. This uncertainty has then been verified over 100 m by comparison with an optical interferometer. The prototype was also tested outdoors over 5.4 km and has shown a resolution of 25 µm for an integration time of 10 ms. Distance measurements for long distances with this prototype are still limited by the air refractive index effect. Nevertheless, we have demonstrated that the uncertainty on optical distances reached with this simple technique is compatible with a future development of a two-wavelength system with air index compensation.**

Index Terms— **Absolute Distance Measurement, Air refractive index, Intensity modulation, Long-distance telemetry, Phase-based distance measurement.**

I. Introduction

Accurate absolute distance measurements over several kilometers are of great interest for several applications such as the construction and surveying of huge structures, for instance dams, colliders [1], tunnels [2], or geological faults [3]. Nowadays, the most accurate commercial optical Absolute Distance Meters (ADMs) used for these applications claim a standard uncertainty of 0.6 mm + 1 ppm up to 1 km (see manufacturers specifications). Nevertheless, in the 1990's, better performances have been reached with the Mekometer ME5000 from the former Kern company [2]. This instrument, no longer manufactured, but still used by several geodetic institutes, can achieve an accuracy (coverage factor, k=1) of 75 µm + 0.5 ppm, i.e. 575 µm at 1 km, with a recording of meteorological conditions at each end of the line, and under favorable atmospheric conditions [2]. However, for distances of several kilometers, millimetric accuracy cannot be reached with classical Electronic Distance Meters (EDM) due to the determination of the air refractive index: an accuracy of 1 mm over 5 km implies a knowledge of the average temperature along the optical path at 0.2 ºC, and of the average pressure at 75 Pa, which is in practice impossible to achieve with classical sensors, especially for air temperature.

To overcome this physical limitation a two-wavelength approach has been early proposed [5] and implemented [6,7]. A commercial version was even manufactured in a few copies in the 1990's [8]. Its physical principle is based on the knowledge of the model of the air index dispersion: measuring simultaneously optical distances with two different wavelengths allows to deduce the geometric distance, without the need to measure air temperature and atmospheric pressure. If we call D the true distance, L_1 and L_2 the optical distances (defined as the product of the geometric lengths by the air indexes n) at the wavelengths λ_1 and λ_2, respectively, D is given by:

$$D = L_1 - \frac{n_1}{n_2 - n_1} \times (L_2 - L_1) \underset{dry\ air}{=} L_1 - A(\lambda_1, \lambda_2) \times (L_2 - L_1) \quad (1)$$

with A a factor independent of atmospheric parameters under assumption of dry air, a limit case giving a good approach of the principle. A only depends on the couple of wavelengths used. Formula (1) shows the price to pay to apply this method efficiently: the A factor amplifies the uncertainty of the difference L_2-L_1. Therefore, to obtain a given uncertainty u_D on the true distance, the optical path difference L_2-L_1 must be determined with an uncertainty A times lower than the targeted uncertainty.

This A factor is equal to 47 for the couple of wavelengths 780 nm / 1550 nm, when group index is relevant [7]. Thus, to obtain a sub-millimetric uncertainty on the true distance for this couple of wavelengths, the uncertainty on the optical path difference L_1-L_2 must be better than 20 µm. This performance is far from being achieved with classical EDM instruments, even when only dealing with the optical distances (i.e. without air index determination), especially for distances of several kilometers. The challenge lies in finding a technical solution enabling a

J. Guillory, D. Truong and J.-P. Wallerand are with Laboratoire commun de métrologie LNE-CNAM, 1 rue Gaston Boissier, 75015 Paris, FR (email: joffray.guillory@cnam.fr).
C. Alexandre is with Centre d'Etudes et de Recherche en Informatique et Communications (CEDRIC), CNAM, 292 rue Saint Martin, 75003 Paris, FR.
M. Teyssendier de la Serve is with Institut National de l'information Géographique et forestière (IGN) , 73 avenue de Paris, 94165 Saint Mandé Cedex, FR.

good compromise between accuracy of optical distance measurements at each wavelength, robustness of the system, cost efficiency and ability to measure over several kilometers, outdoors, in field conditions.

Many techniques have already been implemented for high accuracy optical distance measurements, including two-colour principle. Femto-second lasers have been widely used in recent years, either as high frequency modulators [9,10] or as multiwavelength generators for interferometry [11,12,13,14], time-of-flight measurements [15], or combination of optical interferometry and time-of-flight methods [16]. These techniques can basically resolve one optical wavelength for overcoming fringe ambiguity and so open the way to absolute distance measurements with nanometer accuracy. Nevertheless, they remain expensive and difficult to implement in an instrument made for field measurements. Recently, demonstration of interferometry with simultaneous measurements at two wavelengths, 532 nm and 1064 nm, was realized outdoors, showing sub-millimeter accuracy over 800 m [17].

In this paper, the telemetric system we present is based on the measurement of the RF phase of an intensity-modulated laser diode after propagation in air. The use of fiber-optic components of the telecommunication industry makes possible the production of a compact, easy-to-use and affordable instrument. This work is a first step towards the achievement of an air refractive index compensated system for applications in the field. Fig. 1 and 2 provide an overview of the developed ADM, and of its compact design. We have quantified the different sources of errors of this telemeter when measuring an optical distance, i.e. the product of the air refractive index by the mechanical distance. The resulting uncertainty budget refers to the instrument itself and does not take into account the atmospheric parameters and the mechanical offset of the telemeter.

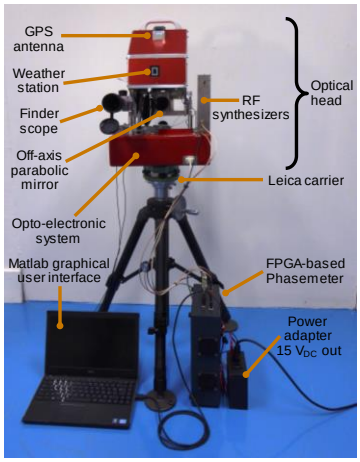

Fig. 1. Photograph of the ADM mounted on a tripod.

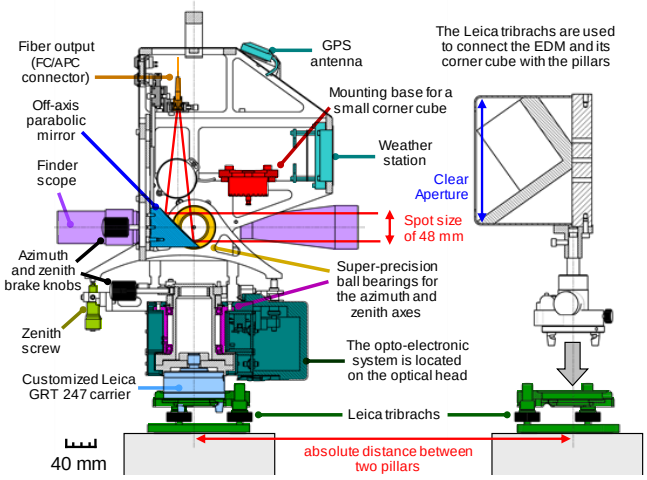

Fig. 2. Cross-section view of the optical head and of a hollow corner cube with a clear aperture of 127 mm.

II. Principle and Implementation of the ADM Prototype.

The ADM is based on the measurement of the phase shift ϕ of a modulation frequency along a measurement path. As shown by formula (2), this phase shift is proportional to the distance L travelled by light:

$$L = \frac{1}{2} \times \left(\frac{\phi}{2\pi} + k \right) \times \frac{c}{n \times f_{RF}} \quad (2)$$

with c the speed of light in vacuum, n the group refractive index of air, f_{RF} the modulation frequency, and k an integer number, called order, and corresponding to the number of times that the phase of the amplitude modulation has rotated by 2π during the propagation.

The operation principle of the telemeter is basically the same as the one described in our previous publication [18].

As depicted in Fig. 3, a 1550 nm optical carrier is emitted by a Distributed FeedBack (DFB) laser diode and intensity modulated by a RF carrier around 5 GHz thanks to a built-in Electro-Absorption Modulator (EAM). This fiber-guided optical signal is then emitted in free space and collimated by an off-axis parabolic mirror for a long-distance propagation: the spot size of 48 mm (at 1 % power level) is reflected back towards the telemeter by a hollow corner cube. The returned signal is finally directed towards a high-speed photodiode and the phase of the photodetected RF signal is measured after a frequency down-conversion at 10.75 MHz. A Variable Optical Attenuator (VOA) sets the optical power received by the photodetector around 50 µW to limit the amplitude to phase coupling effect, as discussed in section III.B)2). Then RF amplification stages adjust the RF power around 0 dBm for optimum operation of the phasemeter. The phase measurement is achieved digitally by a Field Programmable Gate Arrays (FPGA) that integrates each individual phase measurement over 10 ms.

To compensate for phase variations in the fiber-optic and electronic components, a fiber-optic reference distance of around 20 cm is measured every second, then subtracted from the free-space measurement. The switch from this reference path to the measurement one is performed by a fiber-optic

optical switch. It has to be noted that the measurement path also includes 20 cm of optical fiber between the output of this switch and the free-space propagation. Thus, this compensation technique makes the system only sensitive to the difference between the fiber-optic reference path and the same length of fiber path comprised between the optical switch and the fiber end of the measurement path. The efficiency of this drift compensation was tested by heating the whole optical head (including laser diode, frequency synthesizers, optical fibers, …) over 7 °C while measuring a fixed distance of 2 m indoors: a linear drift of 4 µm/°C was recorded. This gives an order of magnitude of the evolution of the mechanical offset with the temperature. A complete study should be conducted subsequently to go towards absolute distance measurements.

The distance measurements in the following sections are always performed using this compensation technique, the switch between the both measurement paths being realized every half second.

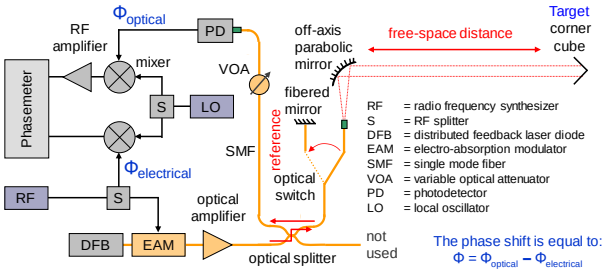

Fig. 3. Functional setup of the ADM.

The procedure for a distance measurement involves three steps, in addition to the measurement of the reference path. First, the order is determined. For this purpose, five different modulation frequencies are used sequentially: 4778 MHz, 4778.01 MHz, 4778.5 MHz, 4839 MHz and 4978 MHz. Thus, five phase shift measurements are obtained, and for each of them, an infinite number of distances according to the value of the order k can be calculated. In order to limit the number of solutions we limit the maximum distance to an arbitrary value of 8 km. The order is the value k for which a common distance exists between each frequency. With this procedure, distance is known within 30 mm, i.e. a half a synthetic wavelength: $c/(n \times f_{RF})$. The time needed for this first step is approximately 10 s, but it can be greatly reduced by a specific design of the FPGA.

In the second step of the distance measurement procedure, a fine measurement of the distance is performed. This consists in measuring the average phase shift over a large number of observations for a modulation frequency of 4895 MHz.

Lastly, when the order and the fine distance have been obtained, the optical distance is corrected from the air refractive index using the Bönsch and Potulski formula [4].

The principle of the developed ADM is finally based on a well-known technique: the phase-based amplitude-modulated light telemetry. This approach is for instance the one applied in the Mekometer ME5000. However, the use of a ten times higher RF carrier than the Mekometer system leads to a better distance resolution according to formula (2) and a lower sensitivity to the crosstalk effect when converted into distance error. Furthermore, adopting up-to-date technologies, such as fiber-optic components not requiring optical alignment and digital electronics providing an efficient signal processing, we can exceed the performances of the Mekometer ME5000 and of the current commercial ADMs, at least for differential measurements (measurement of distance between two positions of a corner cube).

III. SOURCES OF ERROR AND UNCERTAINTY BUDGET OF DIFFERENTIAL OPTICAL DISTANCE MEASUREMENTS

According to formula (2), the optical distance measurement is deduced from a phase shift measurement and the knowledge of the frequency of modulation. In addition, to deduce a geometric distance from the optical distance, the air refractive index through which the optical beam is propagated should be properly determined. The standard uncertainty on the measured distance, u_L, can therefore be separated in two components: $u_{instrument}$, the component coming from the measurement of the optical distance itself and u_n, the component coming from the measurement of air refractive index – which depends on the air temperature, the atmospheric pressure, the partial pressure of water vapor, and the CO_2 content – and from its fluctuations. $u_{instrument}$ can itself be divided in a phase measurement accuracy component u_Φ and in a RF accuracy component u_{fRF}:

$$\left(\frac{u_L}{L}\right)^2 = \underbrace{\left(\frac{u_\phi}{\phi + 2k\pi}\right)^2 + \left(\frac{u_{f_{RF}}}{f_{RF}}\right)^2}_{\text{instrument component}} + \underbrace{\left(\frac{u_n}{n}\right)^2}_{\text{air index component}} \quad (3)$$

In order to state if the uncertainty budget is compatible with a future production of a dispersion-based air index compensated system, only the uncertainty components of the instrument are relevant since only the optical distances are required in formula (1).

A. *Frequency of the modulation: u_{fRF}*

An error in the value of the modulation frequency leads to a scale error in the distance measurement. In practice, the modulation frequency is generated by a synthesizer locked on a miniature Rubidium (Rb) clock (model SA.22c from Microsemi, Application Profile 3) that is specified to have a monthly relative aging rate of $\pm 3 \cdot 10^{-10}$. The frequency of this clock can be compared in our laboratory to a Global Positioning System (GPS) disciplined Rb clock with a relative standard uncertainty of $3 \cdot 10^{-12}$. By measuring yearly the frequency delivered by the frequency synthesizers, a relative uncertainty of the frequency of modulation better than $4 \cdot 10^{-9}$ is ensured.

$$\frac{u_{f_{RF}}}{f_{RF}} = 4 \cdot 10^{-9} \quad (4)$$

B. *Phase measurement: u_Φ*

The phase measurement can be affected by two different sources of systematic measurement error, the crosstalk effects and amplitude to phase coupling. In addition, a random noise

limits the resolution of the telemeter for a given integration time. The systematic measurement errors have been minimized during the design phase of the instrument so that they do not lead to correction. Nevertheless, measurement uncertainty on these errors have been quantified. At the end, the uncertainty on the phase measurement can be expressed as follow:

$$\frac{u_\phi}{\phi + 2k\pi} \times L = \sqrt{u^2_{crosstalk} + u^2_{AM/PM} + u^2_{random}} \quad (5)$$

1) *Crosstalk effect: $u_{crosstalk}$*

A RF leakage of the modulation frequency from the emission stages to the reception ones leads to the addition of a spurious signal to the ideal measurement signal. This leakage, due to poor optical or electromagnetic isolations in some components, and excessive RF radiations from other ones, induces a cyclic error, sinusoidal with the distance, that depends on the relative phase and relative amplitude between the crosstalk and the ideal signal. The period of this cyclic error is equal to half a synthetic wavelength, i.e. 30 mm in practice. The Signal to Crosstalk Ratio (SCR), expressed in dB, is quantified by measuring the amplitudes of the signals at intermediate frequency, i.e. 10.75 MHz, at the phasemeter input, when an optical beam is received, then when it is interrupted. The amplitude (half peak-to-peak) of this cyclic error can be well approximated by:

$$A_{crosstalk}\ [\mu m] = \frac{1}{4\pi} \times \frac{c\ [m/s]}{f_{RF}\ [MHz]} \times 10^{-SCR[dB]/20} \quad (6)$$

As this error is a sine function, its probability density function is an arcsine distribution and its variance is half the square of the amplitude of the periodic error [19]. The uncertainty component due to crosstalk is so:

$$u_{crosstalk}\ [\mu m] = \frac{A_{crosstalk}}{\sqrt{2}} = \frac{1}{\sqrt{2}} \times \frac{1}{4\pi} \times \frac{c}{f_{RF}} \times 10^{-SCR/20} \quad (7)$$

In the developed system, the crosstalk level is typically -75 dBm and the signal level 0 dBm, i.e. a SCR of 75 dB, which corresponds to an uncertainty component of 0.6 µm (k=1).

Experimental verification of formula (7) was realized using an interferometric bench as reference of displacements. The difference between the interferometric distances and the ones given by the ADM was recorded over a distance of one synthetic wavelength, i.e. 61 mm. As depicted in Fig. 4, a dedicated setup was realized to vary the SCR: a fiber-optic splitter was added at the output port of the ADM to direct a part of the modulated light towards another retroreflector. This modulated signal, with a fixed RF phase, was added to the measurement signal in order to simulate a crosstalk. Its amplitude can be changed by slightly misaligning the reflector of the crosstalk path. Finally, for a given configuration, the SCR is stable at ±0.5 dB. As shown in Fig. 5, the high goodness of fit between the experimental curves and the simulated ones shows that formula (6) fully reflects the effect of a crosstalk on the measurement accuracy.

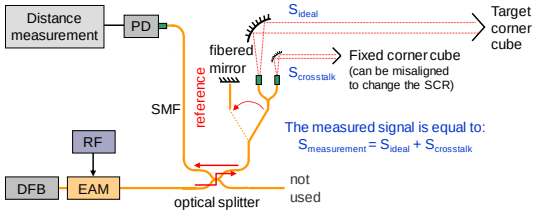

Fig. 4: Experimental setup for the simulation of the crosstalk effect.

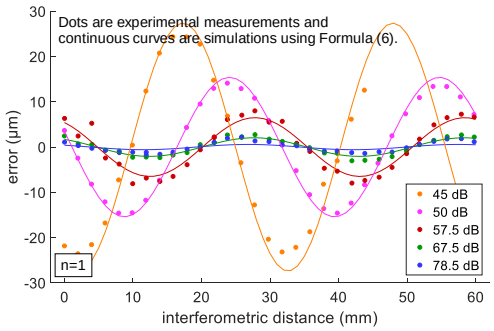

Fig. 5: Non-linearity of the instrument due to the crosstalk effect for different Signal to Crosstalk Ratios (SCR).

2) *Amplitude to phase coupling: $u_{AM/PM}$*

This effect corresponds to a conversion of an intensity variation of the modulated optical signal into a phase variation of the electrical signal generated by the photodetector. This effect has already been studied in previous works [20, 21] with several types of photodetectors: it has been demonstrated that the use of a Positive-Intrinsic-Negative (PIN) photodetector with low optical input power limits the amplitude to phase coupling. Additional power-dependent phase shift can also be generated by the RF components following the photodetector. In that case, the solution consists in using a RF chain working at intermediate frequency as depicted in Fig. 3. In practice, a variation of the RF signal at the phasemeter input due to optical power variation induces a variation of the measured distance as depicted in Fig. 6. A linear variation of the measured distance is observed when the RF power varies from -10 dBm to +5 dBm with a slope of -0.15 µm/dB. When a distance measurement is made with a peak-to-peak power variation of x dB, and assuming a rectangular probability function, the uncertainty associated to the amplitude to phase coupling can be written as:

$$u_{AM/PM}\ [\mu m] = \frac{1}{2\sqrt{3}} \times 0.15\ [\mu m/dB] \times x\ [dB] \quad (8)$$

For long-distance measurements, x is of the order of 10 dB. In that case, $u_{AM/PM}$ is of the order of 0.4 µm (k=1).

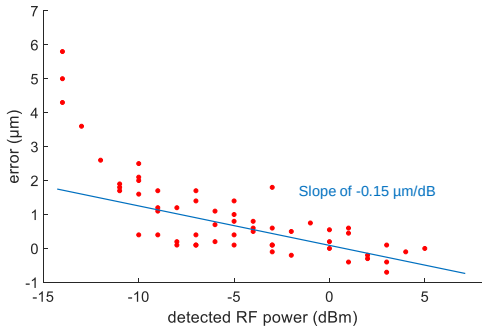

Fig. 6. Variation of the measured distance as a function of the detected RF power at intermediate frequency.

3) Random noise: u_{random}

The standard deviation of a short distance measurement, in a quiet environment without amplitude variation (no amplitude to phase coupling) and without distance variation (no visible crosstalk effect), is 0.8 µm for a sample of 6000 points during 60 s. Using formula (2) to convert distance variations into phase variations for a modulation frequency around 5 GHz, this value corresponds to a phase noise of $2\pi/37500$ for 10 ms of integration time. For comparison to an optical interferometer at 633 nm, this would correspond to a distance noise of 8 pm. Fig. 7 shows this relative distance measurement obtained in laboratory conditions for a distance of 244 mm. This internal random noise is then quantified by:

$$u_{random} = 0.8\mu m \quad (9)$$

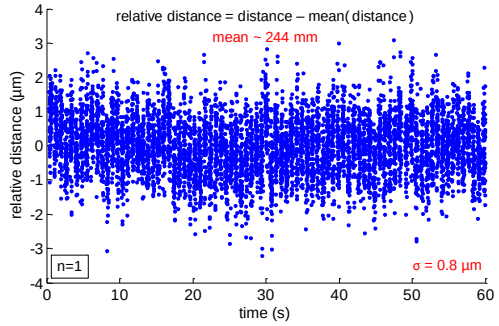

Fig. 7. Relative distance as a function of time. n=1 means that no air refractive index correction was applied.

C. Air refractive index: u_n

The uncertainty on the air refractive index can be classified into two components, $u_{n\ average}$ and $u_{n\ turbulences}$.

The first component, $u_{n\ average}$, is linked to the correction made by the operator. In general, the latter calculates the average air refractive index along the optical path using physical models such as Edlén or Bönsch and Potulski which have an accuracy of $3 \cdot 10^{-8}$. Hence, the uncertainty on the air refractive index will mainly depend on our capacity to measure properly the different atmospheric parameters: the air temperature, the pressure, the partial pressure of water vapor, and the CO_2 content. As indicators, an error of 1 ºC on the measured temperature has an impact of 1 mm/km and an error of 100 Pa on the pressure has an impact of 270 µm/km.

The second component, $u_{n\ turbulences}$, is linked to the dynamic variations in air density. As observed in our measurements, the latter bring a turbulence-induced noise at the instrument level that depends on the measured distance and on the atmospheric conditions.

Outdoors, in quiet atmospheric conditions, we observe a short-term random noise due to the fluctuations of the atmospheric parameters of only 3.3 µm over 864 m, for an integration time of 10 ms for each data point (Fig. 8).

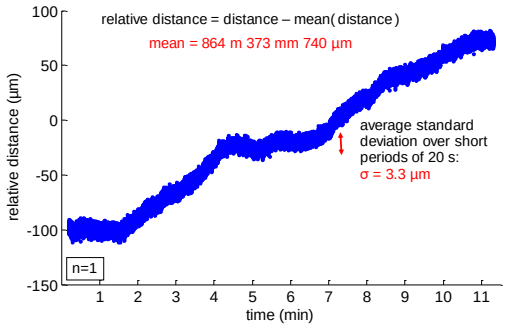

Fig. 8. Data points obtained over 864 m at FGI baseline (Nummela, Finland).

Tests have also been conducted over longer distances, over 4.1 km, in harsh conditions: it was a warm and sunny day with temperatures around 35 °C and important beam scintillations. Under these conditions, as there is no active pointing servo system to keep the optical head on the corner cube, it is necessary to regularly slightly realign the optical head in the vertical direction to optimize the received signal. The results have shown standard deviations up to 40 µm over 20 s of measurement. This is the maximum observed standard variations for such distances.

The extra random noise due to atmospheric turbulences is therefore quantified by values from 3 µm/km in quiet environments to 10 µm/km in harsh conditions:

$$3 \cdot 10^{-9} < \frac{u_{n\ turbulences}}{n} < 10 \cdot 10^{-9} \quad (10)$$

D. Uncertainty budget

A global uncertainty budget for the measurement of a mechanical displacement (distance between two positions of a same reflector) can be formally written, taking into account the different sources of uncertainty listed above, as following:

$$u_L = \sqrt{\frac{u^2_{f_{RF}}}{f^2_{RF}} L^2 + u^2_{crosstalk} + u^2_{AM/PM} + u^2_{random} + \frac{u^2_{n\ average}}{n^2} L^2 + \frac{u^2_{n\ turbulences}}{n^2} L^2}$$

The component coming from the measurement of the optical distance itself, $u_{instrument}$, is obtained by omitting air index components in this expression. It is below 4 µm (k=1) for distances less than 1 km. For a distance of 1 km, peak-to-peak amplitude variations of the signal of 10 dB and a SCR of 75 dB, the uncertainty of the instrument is:

$$u_{instrument} = \sqrt{\frac{u^2_{f_{RF}}}{f^2_{RF}} L^2 + u^2_{crosstalk} + u^2_{AM/PM} + u^2_{random}}$$
$$= \sqrt{\left(4 \cdot 10^{-9} \times 10^9\right)^2 + 0.6^2 + 0.4^2 + 0.8^2}\ \mu m$$
$$= 4.1 \mu m$$

The uncertainty budget of the instrument, excluding air index

determination and mechanical offset of the instrument, is summarized in Table 1.

Standard uncertainty component	Source of uncertainty	Standard uncertainty	Sensitivity coefficient	Contribution
$u_{f_{RF}}$	accuracy of the modulation frequency	$4 \cdot 10^{-9}\ f_{RF}$ Hz	L / f_{RF} m.s	$4 \cdot 10^{-9}\ L$ µm †
$u_{crosstalk}$	value of the signal to crosstalk ratio	$10^{-75/20}$ / $\sqrt{2}$	c / (4π f_{RF}) m	0.6 µm * †
$u_{AM/PM}$	variations of the signal amplitude	10 / $2\sqrt{3}$ dB	-0.15 µm/dB	0.4 µm **
u_{random}	random noise on the phase measurement	0.17 mrad	4.7 µm/mrad	0.8 µm
* for SCR of 75 dB ** for peak-to-peak amplitude variations of 10 dB † for f_{RF} = 5 GHz				
Combined standard uncertainty		$u_{k=1}(L) = \sqrt{(1.1\ \mu m)^2 + (4 \cdot 10^{-9}\ L)^2}$		

Table 1: Uncertainty budget for differential optical distance measurements with the telemeter prototype.

IV. VALIDATION OF THE UNCERTAINTY ESTIMATION AND RANGE OF OPERATION

Validation of the uncertainty budget should be conducted by comparison to a reference system with an uncertainty better than or equivalent to the claimed uncertainty of the developed instrument. This was done up to 100 m using a linear bench whose displacement is measured by a 633 nm interferometer. In that case environmental parameters are well controlled and have a negligible effect on the comparison.

A. Comparison to a 100 m interferometric displacement

The telemeter was compared to a 50m-long interferometric bench, indoors, in a controlled environment. As depicted in Fig. 9, the interferometric beam was propagated over 50 m while the telemeter beam was propagated over 100 m thanks to a double round trip. The interferometric distance has so been multiplied by a factor of two for the comparison.

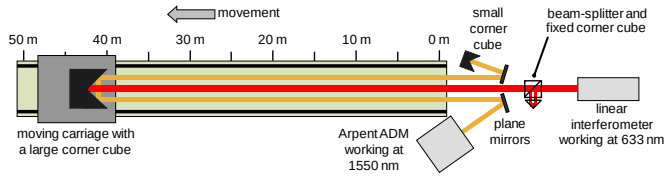

Fig. 9. Setup realized for the comparison between a linear interferometer and the developed ADM.

The difference between twice the interferometric distance at 633 nm and the ADM distance at 1550 nm was lower than 2 µm the first day (versus 8 µm the second day) with a standard deviation of only 1.0 µm (versus 2.2 µm the second day). As both instruments do not operate at the same wavelength, a small error can occur if atmospheric parameters are not properly estimated. Nevertheless, this error is negligible at the micrometer scale: if temperature measurement is made with an error of 1°C, this implies only 100 nm error in the comparison.

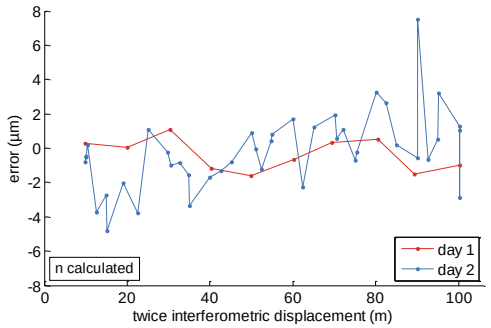

Fig. 10. Error as a function of the interferometric displacement.

During the comparison, the SCR was always higher than 75 dB. Formula (7) shows that in that case the uncertainty component associated to crosstalk is lower than 1.5 µm, which is compatible with the comparison depicted in Fig. 10.

B. Resolution and range of operation outdoors

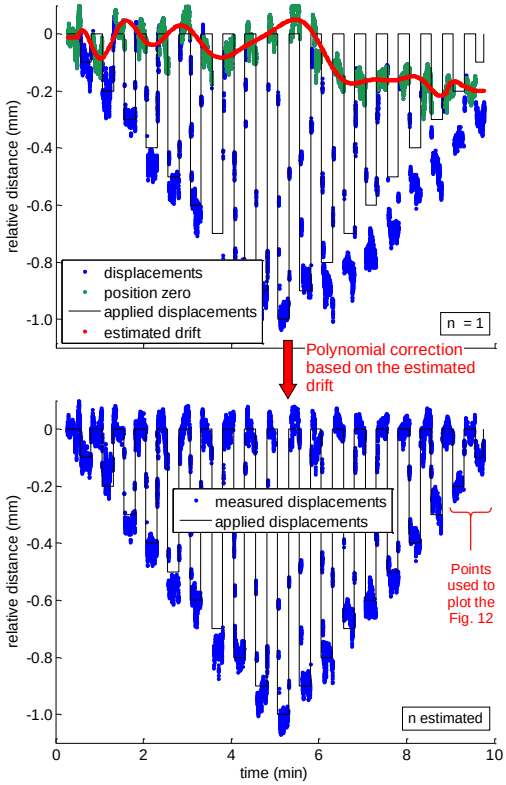

Fig. 11. Measurement of 100 µm steps displacement of the corner cube after a propagation over 5.4 km in air.

The telemeter has been tested over 5.4 km, above an urban area, between the roofs of two buildings located in Paris (LNE building) and nearby Paris (Meudon observatory). Two weather stations were installed at each end of the line: temperatures were 8.2 °C and 10 °C, pressures 1003.6 hPa and 992.9 hPa (the Meudon observatory is located about 80 m above the LNE building), and relative humidities 57 % and 68 % in Paris and Meudon, respectively. The sky was overcast with a ~14 km/h wind. The short term (15 s) sample standard deviations were between 10 µm and 40 µm for 10 ms of integration time for each individual measurement point.

The 5.4 km distant corner cube was moved by steps of 100 µm thanks to a micrometric translation stage, from 0 mm to -1 mm, then from -1 mm to 0 mm. Between each step, additional measurements of the 0 mm position were realized to estimate the distance drift that occurred during the 10 min measurement due to the evolution of the atmospheric parameters. As depicted in Fig. 11, at the top, a polynomial drift has been considered (red curve). A distance variation of 200 µm for 10 minutes, as the one depicted in Fig. 11 (in the plot above), corresponds to a variation of the average temperature along the 5.4 km path of only 0.04 °C, for which drift of the instrument is negligible. At the bottom, we easily distinguish the distance variations despite the atmospheric disturbances.

For each position of the corner cube a distribution of the measured distances can be plotted. In Fig. 12, histograms of the measurement values obtained at the three last positions of Fig. 11 are depicted. We obtain normal distributions with standard deviations between 21 µm and 28 µm. These values correspond to the instrument resolution (1σ) at 5.4 km.

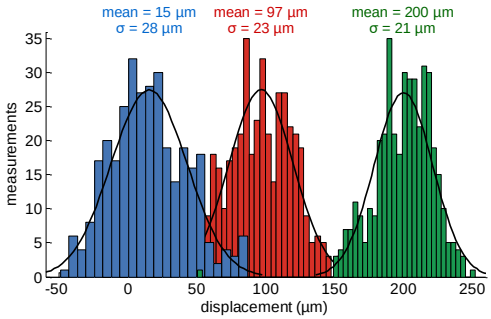

Fig. 12. Distribution of the recorded distances for three corner cube positions.

V. CONCLUSION

We have developed a robust, compact, and easily transportable distance meter.

Indoors, in a controlled environment, its uncertainty for a displacement measurement is around 2 µm (k=1) up to 100 m. Outdoors, in quiet environmental conditions, the measurement resolution is 3 µm (1σ) over 850 m. In field conditions and urban environment, the resolution of the prototype is around 25 µm for 5.4 km of measured distance (10.8 km of propagation). The accuracy of the mechanical distance measured by the prototype is still limited by air index determination along the propagation path of the optical beam. However, the uncertainty obtained for optical path measurement with the prototype is compatible with a future improvement of the setup by the addition of a second wavelength in order to partially compensate the air index effect. This second wavelength could be obtained by frequency doubling of the 1550 nm light. Even if implementation of all fiber-optic system for both wavelengths is more complex, this has already been demonstrated in [22]. In that case millimeter uncertainty on a distance measurement could be reached over 5 km without air temperature and pressure measurement.

ACKNOWLEDGMENT

This work was partially funded within the European Metrology Research Programme (EMRP) as JRPs SIB60 Surveying and IND53 Luminar. The authors are very grateful to J. Cali and S. Durand from École Supérieure des Géomètres et Topographes (ESGT) for the availability of their interferometric bench. They are also very grateful to J. Jokela from Finnish Geospatial Research Institute (FGI) for the availability of their baseline and for his assistance during measurements. First design of the FPGA based phasemeter was realized within the project 7-BLAN-0309-01 of the ANR (French National Agency for Research), coordinated by M. Lintz from Observatoire de la Côte d'Azur.

REFERENCES

[1] J. Gervaise, "First results of the geodetic measurements carried out with the Terrameter, two wavelength electronic distance measurement instrument". Proc. Of Geodätischen Seminar über Electrooptische Präzisionsstreckenmessung, Munich, Germany, pp. 213-229, January 1984. [online] Available: http://doczz.com.br/doc/1162343/schriftenreihe---universit%C3%A4t-der-bundeswehr-m%C3%BCnchen, Accessed on July 3, 2018.

[2] C.J. Curtis, "Calibration and use of the Mekometer ME5000 in the survey of the Channel Tunnel". Proceedings of the Workshop the use and calibration of the Kern ME5000 Mekometer, Stanford Linear Accelerator Center, Stanford University, Stanford, California, USA, pp. 67-82, June 18-19,1992. [online] Available: http://www.slac.stanford.edu/pubs/slacreports/reports03/slac-r-403.pdf, Accessed on July 3, 2018.

[3] USGS Eathquake Hazards Program. "Two-color Electronic Distance Meter (EDM)". [online] Available: https://earthquake.usgs.gov/monitoring/deformation/edm/, Accessed on July 3, 2018.

[4] G. Bönsch and E. Potulski, "Measurement of the refractive index of air and comparison with modified Edlén's formulae", *Metrologia*, vol. 35, n°. 2, pp. 133-139, 1998, DOI: 10.1088/0026-1394/35/2/8.

[5] P. L. Bender and J. C. Owens, "Correction of optical distance measurements for the fluctuating atmospheric index of refraction" *J. Geophys. Res.*, vol. 70, n°.10, pp. 2461-2462, May 1965, DOI: 10.1029/JZ070i010p02461.

[6] K. B. Earnshaw and J. C. Owens, "A dual wavelength optical distance measuring instrument which corrects for air density" *IEEE J. Quantum Electron.*, vol.3, n°.11, pp. 544-550, 1967, DOI: 10.1109/JQE.1967.1074403.

[7] K.B. Earnshaw and E.N. Hernandez, "Two-Laser Optical Distance-Measuring Instrument that Corrects for the Atmospheric Index of Refraction", *Appl. Opt.*, Vol. 11, n°. 4, pp. 749-754, April 1972. DOI: 10.1364/AO.11.000749.

[8] G. R. Huggett, "Two-color terrameter," *Tectonophysics*, vol. 71, pp. 29–39, 1981, DOI. 10.1016/0040-1951(81)90044-5.

[9] N. R. Doloca, K. Meiners-Hagen, M. Wedde, F. Pollinger and A. Abou-Zeid, "Absolute distance measurement system using a femtosecond laser as a modulator", *Meas. Sci. Technol.*, vol. 21, n°11, 7pp, September 2010, DOI: 10.1088/0957-0233/21/11/115302.

[10] K. Minoshima and H. Matsumoto, "High-accuracy measurement of 240-m distance in an optical tunnel by use of a compact femtosecond laser", *Appl. Opt.*, vol. 39, n° 30, pp. 5512-5517, 2000, DOI: 10.1364/AO.39.005512.

[11] S. A. van den Berg, S. T. Persijn, G. J. P. Kok, M. G. Zeitouny and N. Bhattacharya, "Many-Wavelength Interferometry with Thousands of Lasers for Absolute Distance Measurement", *Phys. Rev. Lett.*, vol. 108, n° 18, May 2012, DOI: 10.1103/PhysRevLett.108.183901.

[12] K. Minoshima, K. Arai and H. Inaba, "High-accuracy self-correction of refractive index of air using two color interferometry of optical frequency combs", *Opt. Express*, vol. 19, n°27, pp. 26095–26105, 2011, DOI: 10.1364/OE.19.026095.

[13] H. J. Kang, B. J. Chun, Y. S. Jang, Y. J. Kim and S. W. Kim, "Real-time compensation of the refractive index of air in distance measurement", *Opt.*

Express, vol. 23, n° 20, pp. 26377–26385, 2015, DOI: 10.1364/OE.23.026377.

[14] G. Wu, K. Arai, M. Takahashi, H. Inaba and K. Minoshima, "High-accuracy correction of air refractive index by using two-color heterodyne interferometry of optical frequency combs", *Meas. Sci. Technol.*, vol. 24, n°1, 015203, Dec. 2012, DOI: 10.1088/0957-0233/24/1/015203.

[15] J. Lee, Y.-J. Kim, K. Lee, S. Lee and S.-W. Kim, "Time-of-flight measurement with femtosecond light pulses", *Nat. Photonics*, vol. 4, pp. 716-720, Aug. 2010, DOI: 10.1038/nphoton.2010.175.

[16] I. Coddington, C. Swann, L. Nenadovic and N. Newbury, "Rapid and precise absolute distance measurements at long range", *Nat. Photonics*, vol. 3, pp. 351-356, May 2009, DOI: 10.1038/nphoton.2009.94.

[17] K. Meiners-Hagen, T. Meyer, J. Mildner and F. Pollinger, "SI-traceable absolute distance measurement over more than 800 meters with sub-nanometer interferometry by two-color inline refractivity compensation", *Appl. Phys. Let.*, vol.111, n° 19, 191104, Nov. 2017, DOI: 10.1063/1.5000569.

[18] J. Guillory, R. Smíd, J. García-Márquez, D. Truong, C. Alexandre and J-P. Wallerand, "High resolution kilometric range optical telemetry in air by RF phase measurement", *Rev. Sci. Instrum.*, Vol. 87, n°7, 075105, 2016, DOI: 10.1063/1.4954180.

[19] JCGM 101:2008, "evaluation of measurement data-supplement 1 to the "guide to the expression of uncertainty in measurements"-propagation of distributions using a Monte Carlo method", page 23. [online] Avalailble: https://www.bipm.org/utils/common/documents/jcgm/JCGM_101_2008_E.pdf, Accessed on July 3, 2018.

[20] J. Guillory, J. García-Márquez, C. Alexandre, D. Truong and J-P. Wallerand, "Characterization and reduction of the amplitude-to-phase conversion effects in telemetry", *Meas. Sci. Technol.*, vol. 26, 084006 (7pp), Jul. 2015, DOI: 10.1088/0957-0233/26/8/084006.

[21] D-H. Phung, M. Merzougui, C. Alexandre and M. Lintz, "Phase Measurement of a Microwave Optical Modulation: Characterisation and Reduction of Amplitude-to-Phase Conversion in 1.5 μm High Bandwidth Photodiodes", IEEE Journal of Lightwave Technology, vol. 32, n°20, pp 3759- 3767, March 2014, DOI: 10.1109/JLT.2014.2312457.

[22] J. Guillory, J-P. Wallerand, D. Truong, R. Smíd and C. Alexandre, "Towards kilometric distance measurments with air refractive index compensation", 3rd Joint International Symposium on Deformation Monitoring (JISDM), Vienna, Austria, 30 March - 1 April, 2016. [online] Avalailble: http://www.fig.net/resources/proceedings/2016/2016_03_jisdm_pdf/nonreviewed/JISDM_2016_submission_27.pdf